Aromatic Ring-Forming Reactions of Metastable Diacetylene with 1,3-Butadiene

Caleb A. Arrington,† Christopher Ramos, Allison D. Robinson, and Timothy S. Zwier*

Department of Chemistry, Purdue University, West Lafayette, Indiana 47907-1393

Received: January 6, 1998; In Final Form: March 5, 1998

The primary reactions of the lowest energy triplet states of diacetylene (C_4H_2*) with 1,3-butadiene (C_4H_6) in a helium buffer are characterized with a molecular beam pump−probe technique. Triplet diacetylene is prepared in the early portions of a molecular expansion by laser excitation of the $2^1_0 6^1_0$ band of the $^1\Delta_u \leftarrow X^1\Sigma^+_g$ transition in C_4H_2 at 231.5 nm, which rapidly interconverts to high vibrational levels of the lowest energy triplet surfaces. The subsequent reactions with C_4H_6 are allowed to proceed for 20 μs while the expansion traverses a short ceramic reaction tube or slit channel. Primary products are observed by quenching secondary processes as molecular collisions cease outside the tube. The major photochemical products C_6H_6 and C_8H_6 are detected in a linear time-of-flight mass spectrometer using both vacuum ultraviolet photoionization and resonant two-photon ionization (R2PI). R2PI spectra of the C_6H_6 and C_8H_6 products unambiguously identify them as benzene and phenylacetylene, respectively. Based on deuterium substitution experiments, a mechanism for these ring-forming reactions is proposed. The potential importance of these reactions for forming aromatics in sooting flames and planetary atmospheres is discussed.

I. Introduction

Diacetylene (C_4H_2, H−C≡C−C≡C−H) plays an important role in such diverse settings as planetary atmospheres and combusting fuels. Its infrared (IR) spectrum has been observed in the atmosphere of Titan, one of the moons of Saturn,[1−3] and on Saturn itself.[4] Diacetylene functions in Titan's atmosphere much like ozone does in earth's atmosphere, shielding the lower atmosphere from ultraviolet (UV) radiation from the sun and photochemically reacting to form larger hydrocarbons and nitriles. One of the unsolved mysteries of current photochemical models of Titan is the identification of the molecular carrier(s) responsible for the visible absorbing haze present in the atmosphere.[5−8] Larger poly-ynes formed from the photochemical reactions of diacetylene are one possibility, motivating recent photochemical studies of diacetylene with various hydrocarbons present in abundance on Titan.[9−13] A second potential source of visible absorptions are polyaromatic hydrocarbons (PAHs), but no experimental evidence for benzene or any PAHs on Titan has yet been obtained.

Diacetylene is also one of the most abundant C_4 hydrocarbons in flames, especially those employing unsaturated hydrocarbon fuels such as acetylene.[14−17] C_4H_2 is involved, either directly or indirectly, in several of the proposed aromatic and PAH-forming reactions in flames.[18−22] PAHs are important precursors to the large aggregate carbon structures of soot produced during combustion.[20,21,23,24] Understanding the early mechanistic steps of ring-formation reactions from small hydrocarbons is essential to a complete understanding of the combustion process. As the prototypical aromatic, routes for formation of benzene in flames have received much attention. Among the routes favored by current models is the recombination of propargyl radicals ($2C_3H_3 \rightarrow C_6H_6$).[20,21] Several other routes are thought also to be of importance under certain fuel and flame conditions and are currently a subject of much debate.[22,25]

The role of metastable excited states in the chemistry of small hydrocarbons such as C_4H_2 are now being explored in some detail.[9−13] At issue is whether such reactions can compete, under certain conditions, with free radical routes for forming more complex hydrocarbons in flames or in planetary atmospheres.[13] Preparation of metastable triplet states of C_4H_2 is facilitated by the efficient intersystem crossing that follows UV excitation to the singlet manifold.[26,27] The bulb studies of C_4H_2 by Glicker and Okabe[26] have shown that much of the UV photochemistry of diacetylene occurs out of metastable triplet states. Over the wavelength range from 184 to 254 nm, C_4H_2 reacts with a quantum yield for diacetylene loss of $\Phi = 2.0 \pm 0.5$, but no radical formation was observed. Triplet states 62 and 76 kcal/mol above the ground state (T_1 ($^3\Sigma_u^+$) and/or T_2 ($^3\Delta_u$))[28] are proposed to be responsible for the observed photochemistry. These states are not quenched even under conditions in which the C_4H_2* experiences thousands of collisions with an inert buffer gas. In the study of Glicker and Okabe,[26] the primary products of the bulb studies could not be determined due to rapid polymerization to larger hydrocarbon species. The electronic structure of the reactive triplet states has been theoretically investigated by Karpfen and Lischka.[29] This study indicates that the lowest-energy triplet states are (nominally) cumulene diradicals with unpaired electrons on either end of the carbon chain.

Motivated by the need to better understand the chemistry of the metastable states of C_4H_2, we have recently pursued photochemical studies of diacetylene[9,10] with several small hydrocarbons, including acetylene,[11] ethylene, propene, and propyne.[12] Our work employs a laser-based pump−probe scheme in which the photochemistry is initiated in a short reaction tube attached to a pulsed valve (Figure 1a). Expansion of the gas mixture from the tube quenches further reaction after 10 to 20 μs, enabling the exploration of the early stages of reaction even in a complex mixture in which polymerization would dominate under bulb conditions. The reaction products are then probed using vacuum UV (VUV) photoionization time-of-flight mass spectroscopy (TOFMS).

* To whom correspondence should be addressed.
† Present address: Department of Chemistry, Mercer University, Macon, GA 31207.

S1089-5639(98)00648-3 CCC: $15.00
Published on Web 04/17/1998

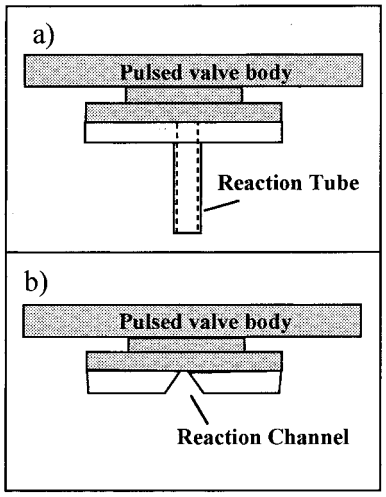

Figure 1. Schematic diagram of the (a) reaction tube and (b) reaction channel used in the present studies of the reaction of metastable diacetylene with 1,3-butadiene.

From such work, C_4H_2* is known to undergo a rich chemistry with unsaturated hydrocarbons. In all cases so far studied, attack by a radical site of C_4H_2* on the π-cloud of an unsaturated hydrocarbon produces a reaction complex that subsequently loses H_2, C_2H_2, or CH_4 (either as intact molecules or as R + H where R = H, CH_3).[9−12]

In the present study, we extend the range of hydrocarbon reaction partners for C_4H_2* to include 1,3-butadiene ($H_2C{=}CH{-}CH{=}CH_2$). The dominant C_4H_2* + C_4H_6 products are C_6H_6 and C_8H_6, which are spectroscopically identified as the aromatics benzene and phenylacetylene ($C_6H_5C{\equiv}CH$), respectively. The reaction thus presents a first example of the ability of metastable diacetylene to undergo ring-forming reactions. The possibility is thereby raised that such reactions could play an unanticipated role in forming aromatics in Titan's atmosphere and in flames.

In Section II, a description of the photochemical apparatus is given. The experimental evidence for the ring-formation reactions is given in Section III and the thermochemistry and mechanism of the reaction are discussed in Section IV. Conclusions are presented in Section V.

II. Experimental Section

Our interest in studying the first steps in the rapid polymerization processes of excited-state diacetylene with unsaturated hydrocarbons has led to the development of a photochemical molecular beam TOF mass spectrometer suited to the purpose. Details of its construction are given in an earlier paper,[10] and aspects specific to the present experiment are included here. Gas mixtures of 1−3% C_4H_2 and 3−10% C_4H_6 in helium are prepared in a stainless steel reservoir. The gas mixture is introduced to the vacuum chamber through a piezoelectric pulsed valve operating at 20 Hz. The total flow rate of the gas is ∼0.02 bar cm^3/s.

To ensure sufficient collisions for the primary reactions while discriminating against subsequent polymerization steps, the reaction mixture is expanded from the pulsed valve either through a short reaction tube or a reaction channel affixed to the orifice of the pulsed valve. The ceramic reaction tube (2 mm inner diameter 8 mm long) constrains the expanding gas mixture at a pressure of a few Torr for the 20-μs time for traversal down the tube before expansion into vacuum (Figure 1a). As the reaction mixture makes this traversal, photochemistry is initiated. The doubled output (0.5 mJ/pulse) of an excimer (XeCl) pumped dye laser operating with Coumarin 460 laser dye is tuned to the $2^1_0 6^1_0$ band of the $^1\Delta_u \leftarrow X^1\Sigma^+_g$ transition in diacetylene,[9] exciting a few percent of the diacetylene molecules. This excited singlet state is a doorway to the reactive triplet state through rapid intersystem crossing, either directly or mediated by the lower-energy $^1\Sigma_u^+$ state, producing high vibrational levels of the lowest energy triplet states.[10,26] Reaction then occurs from this metastable state(s) until molecular collisions cease outside of the reaction tube as the free expansion begins. We estimate that the C_4H_2* molecules undergo ∼100 collisions with buffer gas and tens of collisions with the reactant of choice while in the tube. As we will see, there is evidence for cooling of the photochemical products in the expansion to temperatures of ∼100 K.

In some cases, the reaction tube has been replaced with a simple reaction channel created by two half-circle disks affixed to the pulsed valve, as shown in Figure 1b. The short channel so produced (only 2 mm in depth) allows the photochemical excitation laser to cross the expansion while it is still constrained by the channel. This alternate source configuration tests for the effects of fewer collisions both in making and cooling the photochemical products. It also provides a check against wall effects, which are minimized in the short channel relative to the reaction tube.

The gas mixture exiting from the photochemical source enters the extraction region of a Wiley−Maclaren TOF mass spectrometer. The reactants and photochemical products take ∼70 μs to reach the ionization region of the mass spectrometer 7 cm away from the reaction tube exit.

In the present work, two photoionization schemes are used. First, general, mass-analysis of products is achieved using one-photon VUV photoionization at 118 nm (10.5 eV) produced by tripling the third harmonic of the Nd:YAG laser in xenon gas.[10] This ionization scheme[30] minimizes fragmentation and provides a general means of uniformly ionizing the neutral molecules, producing a mass spectrum that reflects the populations (and photoionization cross sections) of the species in the molecular beam.

Second, in favorable cases, the optical spectrum of the photochemical products is recorded in one-color resonant two-photon ionization (R2PI) using the doubled output of a Nd:YAG-pumped dye laser. In this way, structural information on specific products is provided that extends beyond the mass-to-charge ratio. Put together, the two ionization schemes provide complementary information on the photochemistry of rapidly reacting species.

In the one-meter drift region of the spectrometer the lower mass reactants are pulsed away with an ∼500-V, 2-μs long pulse so that the microsphere plate voltage can be increased to detect the much weaker (∼100 to 200 times) photoproduct ion signal. The ion signal is digitized every 10 ns and displayed by a digital oscilloscope. Data are transferred and stored on a personal computer.

The 1,3-butadiene (99.0%) was used as supplied (Matheson). Diacetylene and deuterated diacetylene were synthesized in our laboratory by procedures described earlier.[10,11] The diacetylene was stored in a gas cylinder as a dilute mixture (∼5%) in helium.

III. Results

A. Vacuum Ultraviolet (VUV) Photoionization Studies. The reaction of C_4H_2* with 1,3-butadiene marks the first C_4 coreactant (other than C_4H_2 itself) studied by our methods. Because C_4H_2* reacts with ground-state diacetylene, the reaction with butadiene occurs in parallel with the C_4H_2* + C_4H_2

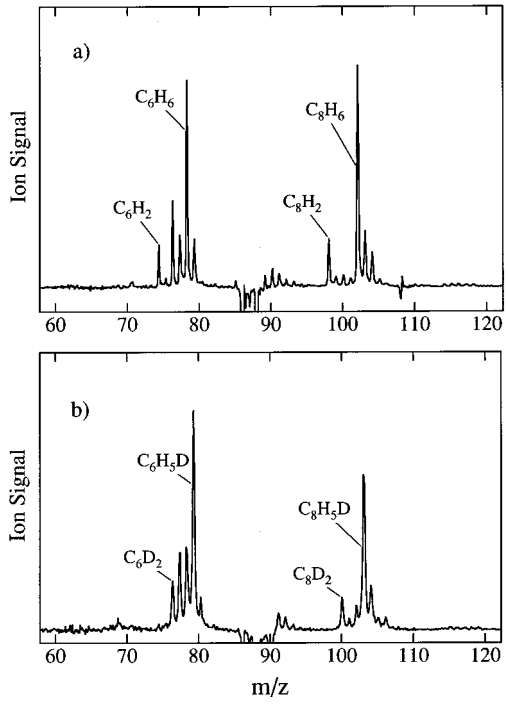

Figure 2. VUV photoionization difference mass spectra (photoexcitation laser off − photoexcitation laser on), highlighting the primary photoproducts of the reactions: (a) $C_4H_2^*$ + C_4H_6 and (b) C_4D_2* + C_4H_6. Products were ionized with 118 nm radiation. The reactant mass peaks (not shown) are ∼200 times larger than those displayed.

reaction. In addition, because the triplet-state diacetylene is formed by intersystem crossing from the singlet manifold following UV excitation, vibrational deactivation of C_4H_2* within the triplet manifold also occurs in parallel with reaction.

Figure 2a presents the VUV photoionization difference TOF mass spectrum of a 1:5 mixture of C_4H_2/C_4H_6 in helium buffer. The spectrum is the difference between a 1000-shot mass spectrum taken with the reactants exposed to the photochemical laser tuned to 231.5 nm (the absorption maximum of the $2^1_0 6^1_0$ band of $^1\Delta_u \leftarrow {}^1\Sigma_g^+$ transition of room temperature diacetylene), and a 1000-shot mass spectrum taken without the photochemistry laser present. The difference spectrum highlights the photochemical products, and also largely compensates for the interference from the impurity 2-chloro-1-butene-3-yne (m/z = 86, 88) present from the synthesis of C_4H_2. The mass signal due to this impurity produces a small negative subtraction that has been shown in earlier work[11] to be photochemically inactive, suggesting a difference in the transport of the gas mixture to the ionization region in the presence of the photoexcitation laser.

Action spectra (not shown) have been recorded by tuning the photoexcitation laser through the $2^1_0 6^1_0$ transition of C_4H_2 while monitoring the photochemical product mass channels. These spectra mimic the absorption spectrum of C_4H_2, proving that photochemical products are only produced when the photoexcitation laser is resonant with the $2^1_0 6^1_0$ transition of C_4H_2. In particular, 1,3-butadiene does not abosrb at 231.5 nm, and no photochemistry is observed in the absence of C_4H_2. The strong singlet UV transitions of C_4H_6 begin at ∼220 nm.[31,32]

The photoproducts displayed in the mass range 60−120 amu are 100 to 200 times smaller than the reactant peaks for C_4H_2 (m/z = 50), C_4D_2 (m/z = 52), and C_4H_6 (m/z = 54) (not shown). In the TOF mass spectra of Figure 2, the photoions are generated with 118 nm VUV radiation. Previous studies[12] of the VUV photoionization of various poly-yne, enyne, and cumulene C_nH_m products have shown no evidence of fragmentation following photoionization at 118 nm. In the present study, VUV photoionization of samples of benzene, phenylacetylene, and styrene also showed negligible fragmentation, indicating that the observed photochemical product ion masses reflect the nascent distribution of neutral species formed in the gas-phase reaction.

The reaction mixture chosen for the difference spectrum of Figure 2a (a 1:5 mixture of C_4H_2/C_4H_6 in a 90% helium balance) favors the C_4H_2* + C_4H_6 reaction over the unavoidable background reaction of C_4H_2 + C_4H_2*. The background self-reaction from previous work is known to produce the photochemical products triacetylene C_6H_2 (m/z = 74) and tetraacetylene C_8H_2 (m/z = 98).[10,33] These masses correspond to loss of C_2H_2 and H_2, respectively, from the C_4H_2* + C_4H_2 reaction complex. Under the conditions used, the C_8H_3 product[10] from C_4H_2* + C_4H_2 is insignificant.

The two dominant product mass peaks in Figure 2a from C_4H_2* + C_4H_6 are m/z = 78 (C_6H_6) and m/z = 102 (C_8H_6), resulting from an analogous loss of C_2H_2 and H_2 from the C_4H_2* + C_4H_6 reaction complex. Minor product channels assignable to C_6H_4, C_6H_5, C_6H_7, C_8H_7, and C_8H_8 are also observed. The full suite of observed reaction channels from the two parallel reactions is, then,

$$C_4H_2^* + C_4H_2 \rightarrow C_6H_2 + C_2H_2 \qquad k_{C_6H_2} \quad (1a)$$

$$\rightarrow C_8H_2 + H_2\ (2H) \qquad k_{C_8H_2} \quad (1b)$$

$$\rightarrow C_8H_3 + H \qquad k_{C_8H_3} \quad (1c)$$

$$C_4H_2^* + C_4H_6 \rightarrow C_6H_6 + C_2H_2\ (C_2H + H) \qquad k_{C_6H_6} \quad (2a)$$

$$\rightarrow C_8H_6 + H_2\ (2H) \qquad k_{C_8H_6} \quad (2b)$$

$$\rightarrow C_6H_4 + C_2H_4 \qquad k_{C_6H_4} \quad (2c)$$

$$\rightarrow C_6H_5 + C_2H_3 \qquad k_{C_6H_5} \quad (2d)$$

$$\rightarrow C_6H_7 + C_2H \qquad k_{C_6H_7} \quad (2e)$$

$$\rightarrow C_8H_7 + H \qquad k_{C_8H_7} \quad (2f)$$

$$+ M \rightarrow C_8H_8 + M \qquad k_{C_8H_8} \quad (2g)$$

Although the intensity of the product signals is about a factor of five less with the reaction channel than the reaction tube, the distribution of products is unchanged, which is consistent with their assignment as primary products of single, gas-phase C_4H_2* + C_4H_6 collisions. The decrease in product intensity when using the reaction channel is also in keeping with the metastable C_4H_2* undergoing fewer collisions in the short reaction channel than in the reaction tube.

To extract from the VUV difference mass spectra the relative product yields, one needs to correct the ion signals for differences in the photoionization cross sections of the products. As we will see in the next section, the two dominant products are benzene and phenylacetylene. Given their chemical similarity, these products are expected to have similar photoionization cross sections. However, the nonaromatic and aromatic products could in principle be quite different. The C_6H_4 product is the most intense of the ion signals from the nonaromatic products. 1-Hexene-3,5-diyne ($H_2C{=}CH{-}C{\equiv}C{-}C{\equiv}CH$) is the likely species responsible for this product signal, which has been spectroscopically identified in other C_4H_2* + alkene reactions.[34]

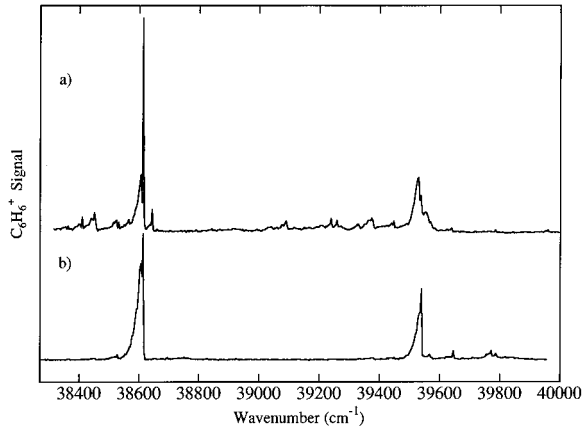

Figure 3. (a) One-color R2PI spectrum of the C_6H_6 photoproduct mass channel. (b) R2PI spectrum of the $S_1 \leftarrow S_0$ transitions of benzene seeded in helium under similar conditions to those used for the photochemistry, identifying the C_6H_6 photoproduct from C_4H_2* + C_4H_6 as benzene.

The photoionization efficiency of the C_6H_4 product relative to the aromatics has not been measured directly because of the difficulty in synthesizing and handling 1-hexene-3,5-diyne. Instead, the relative photoionization cross section is estimated by assuming that C_4H_2 and C_6H_4 have similar photoionization cross sections at 118 nm due to their structural similarity. Mixtures of C_4H_2 and C_6H_6 were made up with known concentration ratios and submitted to VUV photoionization. From such measurements, the ratio of photoionization cross sections at 118 nm was determined to be: $\sigma(C_6H_6)/\sigma(C_4H_2) = 1.05 \pm 0.10$. Assuming the same ratio for $\sigma(C_6H_6)/\sigma(C_6H_4)$, the relative product yields of $C_6H_6/C_8H_6/C_6H_4$ are 0.93 ± 0.08: $1.00{:}0.38 \pm 0.07$.

Difference mass spectra of isotopically labeled reactants have been recorded to provide additional insight to the reaction mechanism. The difference mass spectrum obtained for the reaction of C_4D_2* with C_4H_6 is shown in Figure 2b. The $2^1_0 6^1_0$ band of the $^1\Delta_u \leftarrow X^1\Sigma^+_g$ transition in C_4D_2 is not significantly shifted from that due to C_4H_2 (231.5 nm).[27] The most notable result of diacetylene deuteration is that the C_6H_6 and C_8H_6 products from C_4H_2* + C_4H_6 are quantitatively shifted up one mass channel in C_4D_2* + C_4H_6, forming almost exclusively the C_6H_5D and C_8H_5D products, respectively.

In addition, comparison of Figures 2a and 2b point to C_6H_3D ($m/z = 77$) as the major $C_6H_nD_m$, $n + m = 4$ product produced from C_4D_2* + C_4H_6. However, the mass 78 product could have a contribution from $C_6H_2D_2$ that cannot be distinguished from the C_6H_4D product of the same mass.

B. R2PI Detection of Products. To assess the structure of the C_6H_6 and C_8H_6 products formed from C_4H_2* + C_4H_6, R2PI scans of these product mass channels were carried out. In the $C_6H_6^+$ mass channel, strong absorptions were found in the 260 nm region (Figure 3a). When compared with the spectrum of benzene taken under similar flow conditions (Figure 3b), the identification of the C_6H_6 product as benzene is unequivocal. The 6^1_0 and $6^1_0 1^1_0$ transitions of benzene labeled in the spectrum are strong vibronically induced transitions of benzene.[35] Despite being a mild expansion, the photochemical products are nevertheless cooled significantly in the expansion from the reaction tube. The spectrum is remarkably devoid of vibrational hot bands given the potential for significant vibrational excitation in the products. Furthermore, the rotational band contour of the benzene product (Figure 4a) is best fit by a 100 ± 50 K rotational temperature Boltzmann distribution (Figure 4b).

The analogous R2PI spectrum recorded for the C_8H_6 mass product is shown in Figure 5a and compared with the spectrum

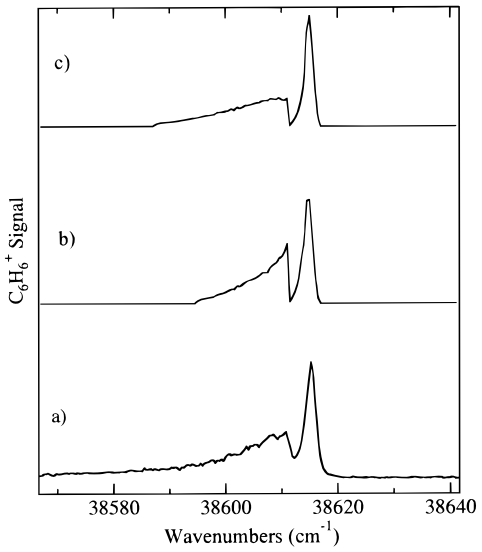

Figure 4. (a) R2PI spectrum of the rotational band contour of the 6^1_0 transition of the benzene produced in the C_4H_2* + C_4H_6 reaction. (b) and (c): Simulated spectra of benzene at $T_{rot} = 50$ K and $T_{rot} = 100$ K, respectively.

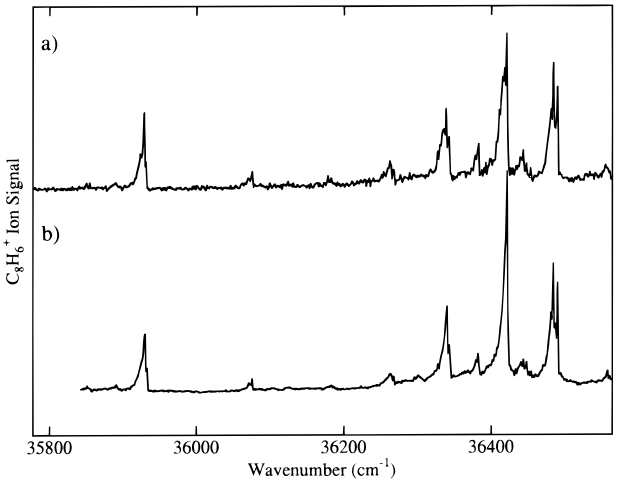

Figure 5. (a) One-color R2PI spectrum of the C_8H_6 photoproduct mass channel. (b) R2PI spectrum of the $S_1 \leftarrow S_0$ origin region of phenylacetylene seeded in helium under similar conditions to those used for the photochemistry, identifying the C_8H_6 photoproduct from C_4H_2* + C_4H_6 as phenylacetylene.

of phenylacetylene below it (Figure 5b). The relative intensities of the R2PI transitions are effected by the close proximity of the two-photon energy to the ionization threshold of phenylacetylene (8.81 eV). Nevertheless, the match provides a firm assignment of the C_8H_6 product as phenylacetylene. As with benzene, no hot bands are observed in the spectrum, indicating significant cooling in the expansion.

Despite being a minor product, the C_8H_8 product that is the stabilized adduct of the C_4H_2* + C_4H_6 reaction also possesses a clean, well-structured R2PI spectrum. Figure 6a presents the photochemical product R2PI spectra of C_8H_8 taken with the reaction tube. The spectrum of styrene (not shown) taken with similar flows of a 2% styrene in helium mixture through the reaction tube, confirms the assignment of the C_8H_8 product as styrene. Unlike benzene and phenylacetylene, significant excitation in the low-frequency out-of-plane torsional modes of styrene (ν_{41} and ν_{42}) is observed in the spectrum. These transitions also dominate the absorption spectrum of room-temperature styrene.[36]

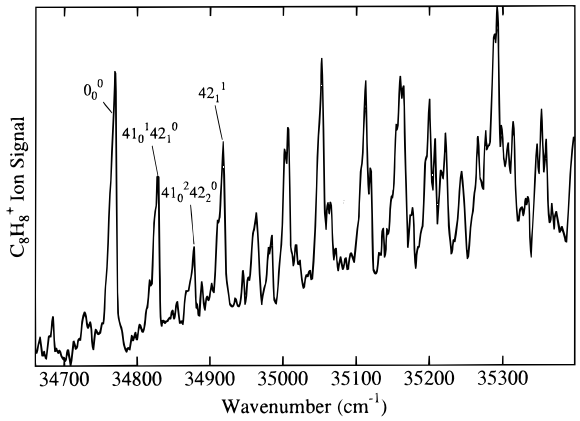

Figure 6. One-color R2PI spectrum of the minor C_8H_8 photoproduct mass channel which is the adduct of the C_4H_2* + C_4H_6 reaction taken with the reaction tube. Assignments of the transitions to individual vibronic bands in the $S_1 \leftarrow S_0$ transition of styrene are taken from ref 35.

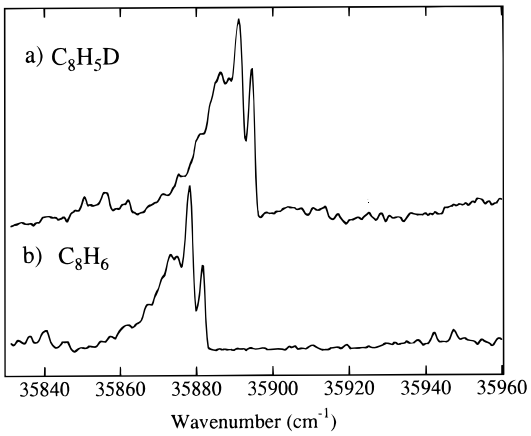

Figure 7. Scans of the phenylacetylene 0^0_0 spectral region in (a) the C_8H_5D mass channel and (b) in the C_8H_6 mass channel for comparison. The C_8H_5D spectrum shows exclusive isotopic substitution for the acetylenic hydrogen from the reaction C_4D_2* + $C_4H_6 \rightarrow C_8H_5D$ + HD.

Similar R2PI scans of the C_8H_8 adduct taken with the reaction channel show the expected changes associated with the decreased number of collisions in this source relative to the reaction tube. First, the C_8H_8 ion signal is five times less intense relative to other products with the reaction channel, indicating less collisional stabilization of the C_8H_8 adduct. Second, the C_8H_8 produced with the reaction channel shows significantly greater vibrational excitation, consistent with a lesser degree of vibrational cooling of the adduct with the reaction channel than the reaction tube.

The power of R2PI spectroscopy in product identification is clearly seen in the spectrum of the C_8H_5D produced from the C_4D_2* + C_4H_6 reaction. Spectra of the C_8H_5D and C_8H_6 species near the phenylacetylene S_1 origin band are shown in Figures 7a and b, respectively. King and So[37] have recorded the optical spectrum for phenylacetylene and deuterated phenylacetylene. They observe a 13 cm^{-1} blue shift from the undeuterated origin band for C_8H_5D when the deuterium is in the acetylenic position, whereas C_8H_5D deuterated in any of the positions on the phenyl ring results in a 31 cm^{-1} blue shift of the origin band. It is clear from the spectra of Figure 7 that C_8H_5D, shifted by 13 cm^{-1}, is exclusively due to photochemical products in which deuterium is in the acetylenic position. This selective deuteration provides a significant constraint on any mechanism developed for the ring-forming reactions (*Section IV*).

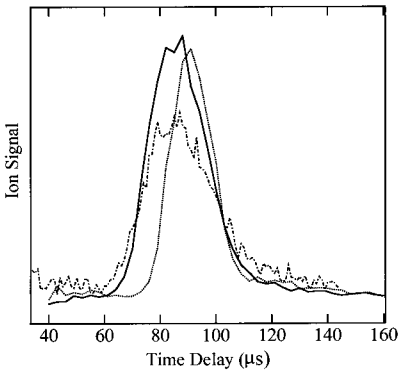

Figure 8. Arrival time scans of (−·−) the C_8H_2 product from C_4H_2* + C_4H_2, (—) the C_8H_6 product from C_4H_2* + C_4H_6 taken with the reaction tube, and (···) the C_8H_6 product taken with the reaction channel.

We have not attempted to record R2PI spectra of the other minor products.

C. Arrival Time Scans. Arrival time scans of all products formed from C_4H_2* + C_4H_6 have been recorded by scanning the delay of the VUV laser relative to the photoexcitation laser pulse. Representative scans of the C_8H_2 product from C_4H_2* + C_4H_2 and the benzene product from C_4H_2* + C_4H_6 taken with the reaction tube and reaction channel are shown in Figure 8. The arrival time distribution of benzene and phenylacetylene are unchanged under VUV or R2PI detection. With either source, the reaction products appear only in a narrow time window associated with the traversal time of the C_4H_2* in the 8-mm tube or 2-mm channel. As expected, the perpendicular excitation geometry and shorter channel length in the latter case produce a narrower distribution of arrival times ($\sim$10 μs). The similarity of the arrival time distributions for benzene and phenylacetylene (not shown) to that for the C_8H_2 product of the C_4H_2* + C_4H_2 reaction is further evidence that benzene and phenylacetylene are formed in a single reactive encounter between C_4H_2* and 1,3-butadiene.

D. Relative Rate Constants. Although the sources used in these studies are well suited to detection of the primary products from C_4H_2* reactions, the pressures and flow velocites are not well characterized enough to allow absolute rate constant measurements. Nevertheless, because secondary reactions are largely quenched by our methods, we have previously used[11,12] a simple pseudo-first-order kinetic scheme to measure effective rate constants for the reactions of C_4H_2* with acetylene, ethene, propyne, and propene relative to the C_4H_2* + C_4H_2 reaction. Using similar reasoning, the kinetic scheme of reactions 1 and 2 predict a linear plot of the integrated intensity ratios of the products of C_4H_2* + C_4H_6 to C_4H_2* + C_4H_2 as a function of the concentration ratio $[C_4H_6]/[C_4H_2]$. In all reactions so far studied, a linear plot has indeed been observed.

The results of such a concentration study for the C_4H_2* + C_4H_6 reaction are plotted in Figure 9 where the concentration of $[C_4H_6]/[C_4H_2]$ is varied from 1:5 to 5:1. Because the corrections for differences in photoionization cross sections of the major products are negligible (*Section III. A*), the slope of the plot gives directly a relative rate constant ratio $k_{C_4H_6}/k_{C_4H_2} = 1.21 \pm 0.07$, reported to one standard deviation.

The relative rate constant for the reaction of C_4H_2* with butadiene is several times larger than that of any of the C_2 or C_3 hydrocarbons so far studied,[10−12] but is comparable in size to the only other C_4 coreactant studied; namely, C_4H_2 itself. One might surmise on this basis that the increased collision cross section of the C_4 species is in large measure responsible for the

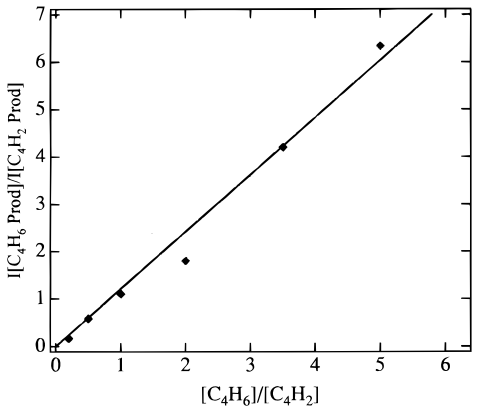

Figure 9. Plotted are the ratios of the ion products intensities $I(C_4H_6$ products$)/I(C_4H_2$ products) versus the reactant concentrations $[C_4H_6]/[C_4H_2]$. The slope of the line fit to these points gives the relative rate constant for the reactions, $C_4H_2^* + C_4H_6 \rightarrow$ products and $C_4H_2^* + C_4H_2 \rightarrow$ products, $k_{C_4H_6}/k_{C_4H_2} = 1.21 \pm 0.07$.

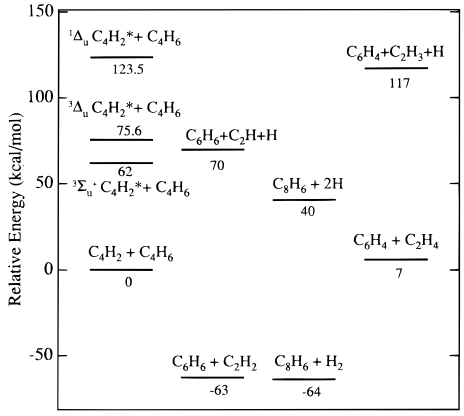

Figure 10. Plotted are the relative reactant and product energies for the major photoproducts formed in the reaction $C_4H_2^* + C_4H_6$. Due to the thermodynamic stability of benzene, the formation of $C_2H + H$ is energetically possible. Thermodynamic quantities are from ref 39.

increased rate rather than any reaction-specific dynamic or steric constraints.

IV. Discussion

The most important result of the present study is the evidence it presents that metastable triplet-state diacetylene reacts with butadiene to form the aromatic products benzene, phenylacetylene, and (in minor amounts) styrene. All the available experimental data support the contention that these products arise from a single reactive collision between $C_4H_2^*$ and C_4H_6.

The Energetics of the Reactions. Figure 10 presents an energy level diagram for the relevant states of the reactants and the major product channels involving formation of C_6H_6, C_8H_6, and C_6H_4. The $^3\Delta_u$ and $^3\Sigma_u^+$ metastable states responsible for the observed chemistry are formed in the present study by intersystem crossing following excitation of the 2^16^1 level of the $^1\Delta_u$ state, 123 kcal/mol above the ground state. Reaction then occurs in parallel with vibrational deactivation in the triplet manifolds.

The triplet states themselves have been observed by electron energy-loss spectroscopy[28] and, more recently by our group[38] in optical spectroscopy using cavity ringdown methods. The vibronic transitions observed in the cavity ringdown experiment are assigned to the lower member of the Renner−Teller couple with symmetry $^3\Delta_u$ in the linear geometry. The (presumed) origin of the accessed excited state is located 75.6 kcal/mol above the ground state (Figure 10). The T_1 state correlating with $^3\Sigma_u^+$ in the linear configuration is tentatively assigned by Allan[28] at an energy of 62 kcal/mol above the ground state.

As Figure 10 shows, the thermodynamic stability of the aromatic products is such that their production from $C_4H_2 + C_4H_6$ is highly exothermic even from ground-state reactants. This result is evident when contrasting the aromatic products with the chain-forming $C_6H_4 + C_2H_4$ product channel some 70 kcal/mol above the aromatic asymptotes. One consequence of the thermodynamic stability of benzene and phenylacetylene is that the reaction asymptotes which form $C_2H + H$ and 2H are also energetically open:

$$C_4H_2^* + C_4H_6 \rightarrow C_6H_6 + C_2H + H \qquad (2a')$$

$$\rightarrow C_8H_6 + 2H \qquad (2b')$$

The corresponding channel forming $C_6H_4 + C_2H_3 + H$ is not open, even if the full 123 kcal/mol excitation energy were available in the colliding reactants.

The R2PI spectra of both C_6H_6 and C_8H_6 show remarkably little internal energy in the benzene and phenylacetylene products (Figures 3a and 5a), essentially reproducing the spectra obtained when benzene and phenylacetylene are expanded from the reaction tube in the absence of photoexcitation (Figures 3b and 5b). One possibile explanation is that benzene and phenylacetylene are formed only from reactions 2a′ (producing $C_2H + H$) and 2b′ (producing 2H), thereby reducing the reaction exothermicity by >100 kcal/mol. Our VUV ionization (10.5 eV) is insufficient to ionize C_2H (11.61 eV), so this intriguing pathway has not been verified.

The more likely explanation is simply that the postreaction tube expansion cools the aromatic products prior to R2PI detection. Treating the exit of the reaction tube (D = 2 mm) as the orifice of a supersonic expansion ($P \sim 2$ Torr), a terminal translational temperature of 20 K is predicted, which is consistent with the 100 K rotational band contour observed for the benzene product (Figure 4). One can assume, then, that vibrational cooling of the products is also occurring, as is apparent from the lack of hot band structure in the observed spectra of Figures 3 and 5.

Reaction Mechanisms. In seeking a reaction mechanism for the aromatic ring-forming reactions, two aspects of the experimental data seem particularly relevant. First, the benzene and phenylacetylene products are formed with similar yields. This result suggests a concerted loss of H_2 or C_2H_2 from the reaction complex rather than successive loss of two H atoms or of $C_2H + H$. The difference in reaction exothermicity (30 kcal/mol) of these latter channels should greatly favor formation of C_8H_6 over C_6H_6. Second, the $C_4D_2^* + C_4H_6$ reaction produces exclusively C_6H_5D and $C_6H_5C{\equiv}CD$ products.

Figure 11a presents a mechanism consistent with the experimental data. The scheme follows aspects of the pathway formulated by Huntsman et al.[39] to account for the thermal aromatization reactions of 1,2,5-trienes. The metastable $C_4H_2^*$ is written as a cumulene diradical, in keeping with the description of Karpfen and Lischka[29] of the $^3\Delta_u$ and $^3\Sigma_u^+$ states from their ab initio calculations. Following attack of $C_4H_2^*$ on 1,3-butadiene, the adduct **1** is formed. The interior double bonds in the cumulene portion of the molecule are in an analogous configuration to the 1,2,5-triene of Huntsman et al.[39] Ring closure then produces the resonance-stabilized cyclopentene **2**. A 1,2-deuterium shift forms the triplet dihydrofulvene intermediate **3**. If intersystem crossing to the singlet state of **3**

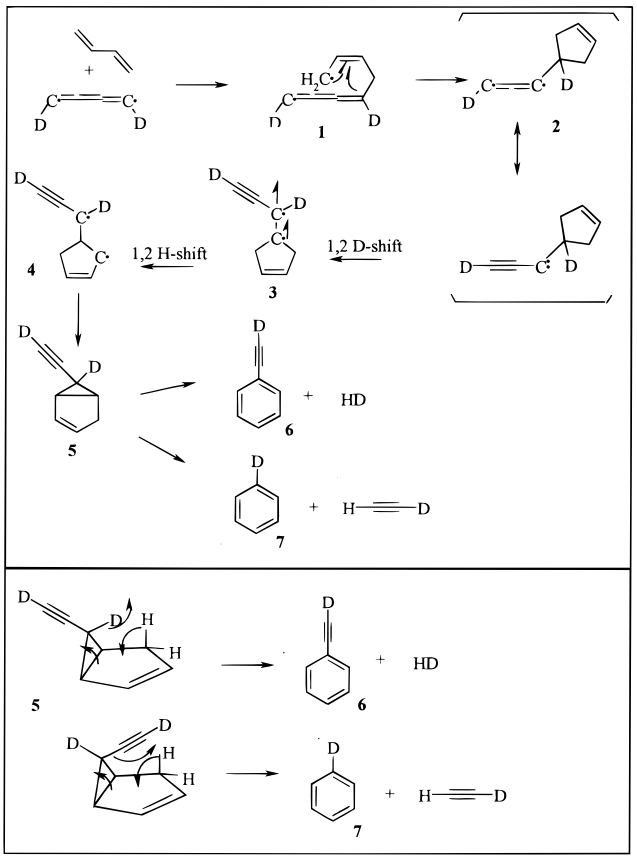

Figure 11. (a) Proposed reaction mechanism for forming singly deuterated benzene and phenylacetylene in similar yields in the reaction of triplet C_4D_2* with 1,3-butadiene. (b) The bicyclohexene intermediate in the reaction mechanism, which, upon stereochemical equilibration, would form the desired products **6** and **7** in comparable yields.

would occur, a dihydrofulvene would be formed which, upon ring-opening, would produce the C_8H_8 chain structure:

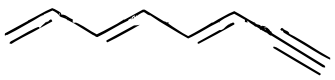

This structure could not aromatize except by a chain process involving successive loss of C_2H (C_2D) and H (D). On energetic grounds (Figure 10), one would anticipate a much greater propensity for phenylacetylene formation over benzene if this route were significant.

An alternative pathway is initiated by a second 1,2 H-shift from **3** to produce the more stable conjugated diradical **4**, whose radical sites are those needed for formation of the key bicyclohexene intermediate **5**. Huntsman and co-workers[39] have observed efficient formation of aromatics from the pyrolysis of bicyclohexenes. As shown in Figure 11b, if stereochemical equilibration of **5** is complete, loss of the endo C_2D or D atoms leads to the desired isotopically labeled phenylacetylene (**6**) and benzene (**7**) products with similar propensities, as required.

The nature of the minor products formed in the $C_4H_6 + C_4H_2$* reaction deserves brief comment. The largest of these minor products is C_6H_4 ($m/z = 76$), which is a photochemical product that we have also observed in the reactions of metastable diacetylene with the other alkenes ethylene ($C_4H_2 + C_2H_4 \rightarrow C_6H_4 + H_2$) and propene ($C_4H_2 + CH_3CHCH_2 \rightarrow C_6H_4 + CH_4$).[12] The structure of the C_6H_4 product in both of these examples has been shown to be 1-hexene-3,5-diyne ($H_2C{=}CH{-}C{\equiv}C{-}C{\equiv}CH$) from its R2PI spectrum.[34] In the analogous

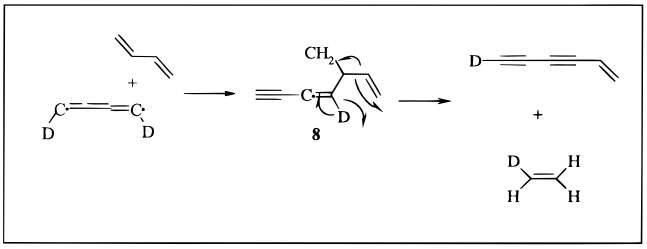

Figure 12. Proposed reaction mechanism for forming the minor product 1-hexene-3,5-diyne (C_6H_4) in the reaction of triplet C_4D_2* with 1,3-butadiene.

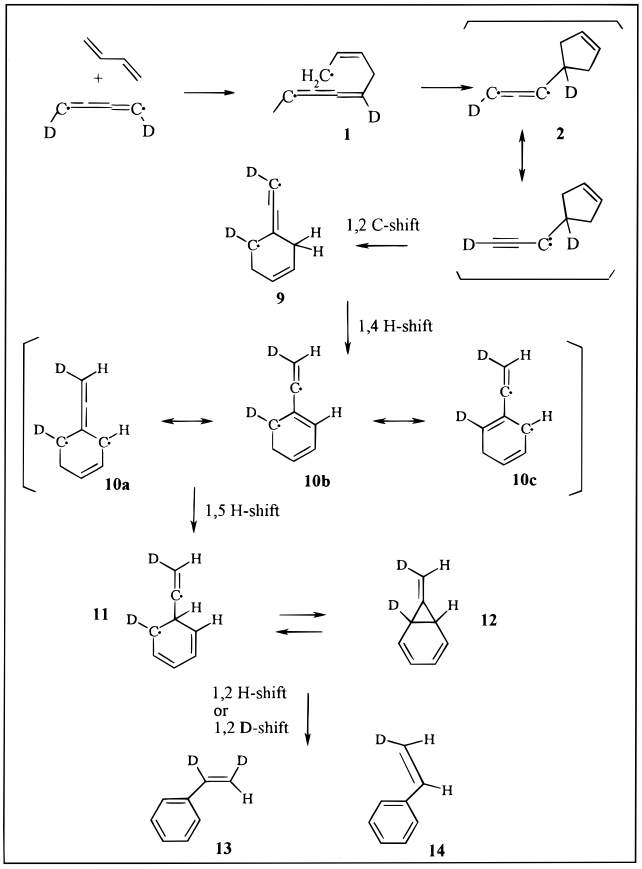

Figure 13. Proposed reaction mechanism for forming the minor adduct styrene in the reaction of triplet C_4D_2* with 1,3-butadiene.

reaction with 1,3-butadiene (Figure 12), attack by C_4H_2* (C_4D_2*) on an interior carbon of 1,3-butadiene produces the reaction complex **8**, from which C_2H_4 (C_2H_3D) is eliminated to form C_6H_4 (C_6H_3D). It is possible that the C_6H_5 mass is formed by an analogous route with loss of only C_2H_3 from the complex. In this case, $C_6H_3D_2$ would be formed in the C_4D_2* + C_4H_6 reaction, consistent with the increased intensity in the m/z 79 mass peak compared with m/z 103 (Figure 1b).

The other minor product for which we have spectroscopic data beyond its mass-to-charge ratio is the C_8H_8 adduct, which we have shown to be styrene. Figure 13 presents a route to its formation that is plausible, but experimentally unverified. If the cyclopentene intermediate **2** undergoes a 1,2 C shift to form **9**, a subsequent 1,4 H shift produces the resonance-stabilized diradical **10**. The substituted trimethylene methane intermediate **10b,c** can then undergo a facile 1,5 H shift to the cyclohexadienyl diradical **11**. If **11** closes to form the bicyclohexadiene **12**, ring opening followed by a final 1,2 H or D shift would produce styrene.

V. Conclusion

In the present work, aromatic ring-forming reactions of metastable diacetylene with 1,3-butadiene have been observed and characterized. Lacking absolute kinetic data, firm quantitative estimates of the importance of these reactions in the atmospheres of the outer planets and moons and in sooting flames is still some time away. Nevertheless, that such reactions form aromatic products in a single reactive collision is noteworthy and intriguing. The reaction mechanisms put forward in the previous section are consistent with the data, but will need to stand up to further tests before they are considered definitive.

A recent estimate[13] suggests that, in the atmosphere of Titan, the metastable states of C_4H_2 (formed by intersystem crossing following absorption of UV solar radiation) may compete with radical reactions as routes to larger hydrocarbons in Titan's atmosphere. The Huygens probe on the current Cassini mission to Saturn will greatly increase the sensitivity of detection of new species in Titan's atmosphere and aerosols. The present study raises the possibility that among the new species to be detected will be aromatic hydrocarbons, including benzene and phenylacetylene.

The high concentration of C_4H_2 often found in sooting flames suggests that metastable diacetylene reactions might also be relevant there. The lower energy of the triplet states of C_4H_2 relative to the triplet states of smaller hydrocarbons, such as C_2H_2, heightens this possibility. Given the importance of ring-forming reactions to soot formation, the formation of benzene and phenylacetylene as dominant products of the $C_4H_2^* + C_4H_6$ reaction is noteworthy, and argues for further investigation of the spectroscopy and chemistry of triplet states of small hydrocarbons such as C_4H_2.

Acknowledgment. The authors gratefully acknowledge the Department of Energy and the NASA Planetary Atmospheres program for their support of this research. The authors also acknowledge the many useful discussions with John Grutzner and Bob Squires on plausible reaction mechanisms for these reactions.

References and Notes

(1) Kunde, V. J.; Aiken, A. C.; Hanel, R. A.; Jennings, D. E.; Maguire, W. C.; Samuelson, R. E. *Nature* **1981**, *292*, 686−688.
(2) Coustenis, A.; Bezard, B.; Gautier, D. *Icarus* **1991**, *80*, 54−76.
(3) Coustenis, A.; Bezard, B.; Gautier, D.; Marten, A.; Samuelson, R. *Icarus* **1991**, *89*, 152−167.
(4) Graauw, T. D.; Feuchtgruber, H.; Bezard, B.; Drossart, P.; Encrenaz, T.; Beintema, D. A.; Griffin, M.; Heras, A.; Kessler, M.; Leech, K.; Lellouch, E.; Morris, P.; Roelfsema, P. R.; Roos-Serote, M.; Salama, A.; Vandenbussche, B.; Valentijn, E. A.; Davis, G. R.; Naylor, D. A. *Astron. Astrophys.* **1997**, *321*, L13-L16.
(5) Yung, Y. L.; Allen, M.; Pinto, J. P. *Astrophys. J. Suppl. Ser.* **1984**, *55*, 465.
(6) Yung, Y. L. *Icarus* **1987**, *72*, 468−472.
(7) Strobel, D. F.; Summers, M. E.; Zhu, S. *Icarus* **1992**, *100*, 512−526.
(8) Toublanc, D.; Parisot, J. P.; Brillet, J.; Gautier, D.; Raulin, F.; McKay, C. P. *Icarus* **1995**, *113*, 2−26.
(9) Bandy, R. E.; Lakshminarayan, C.; Frost, R. K.; Zwier, T. S. *Science* **1992**, *258*, 1630−1633.
(10) Bandy, R. E.; Lakshminarayan, C.; Frost, R. K.; Zwier, T. S. *J. Chem. Phys.* **1993**, *98*, 5362−5374.
(11) Frost, R. K.; Zavarin, G.; Zwier, T. S. *J. Phys. Chem.* **1995**, *99*, 9408−9415.
(12) Frost, R. K.; Arrington, C. A.; Ramos, C.; Zwier, T. S. *J. Am. Chem. Soc.* **1996**, *118*, 4451−4461.
(13) Zwier, T. S.; Allen, M. *Icarus* **1996**, *123*, 578−583.
(14) Bastin, E.; Delfau, J.-L.; Reuillon, M.; Vovelle, C.; Warnatz, J. *Twenty-second Symposium (International) on Combustion*, Pittsburgh, PA, 1988; pp 313−322.
(15) Lam, F. W.; Howard, J. B.; Longwell, J. P. *Twenty-second Symposium (International) on Combustion*, Pittsburgh, PA, 1988; pp 323−332.
(16) Melius, C. F.; Miller, J. A.; Evleth, E. M. *Twenty-fourth Symposium (International) on Combustion*, Pittsburgh, PA, 1992; pp 621−628.
(17) Miller, J. A.; Melius, C. F. *Combust. Flame* **1992**, *91*, 21−39.
(18) Westmoreland, P. R.; Dean, A. M.; Howard, J. B.; Longwell, J. P. *J. Phys. Chem.* **1989**, *92*, 8171−8180.
(19) Lindstedt, R. P.; Skevis, G. *Combust. Flame* **1994**, *99*, 551−561.
(20) Marinov, N. M.; Pitz, W. J.; Westbrook, C. K.; Castaldi, M. J.; Senkan, S. M. *Combust. Sci. Technol.* **1996**, *116*, 211−287.
(21) Castaldi, M. J.; Marinov, N. M.; Melius, C. F.; Huang, J.; Senkan, S. M.; Pitz, W. J.; Westbrook, C. K. *Twenty-sixth Symposium (International) on Combustion*, Pittsburgh, 1996.
(22) Melius, C. F.; Colvin, M. E.; Marinov, N. M.; Pitz, W. J.; Senkan, S. M. *Twenty-sixth Symposium (International) on Combustion*, Pittsburgh, 1996.
(23) Lafleur, A. L.; Howard, J. B.; Marr, J. A.; Yadav, T. *J. Phys. Chem.* **1993**, *97*, 13539−13543.
(24) Lafleur, A. L.; Taghizadeh, K.; Howard, J. B.; Anacleto, J. F.; Quilliam, M. A. *J. Am. Soc. Mass Spectrom.* **1996**, *7*, 276−286.
(25) Lindstedt, R. P.; Skevis, G. *Twenty-sixth Symposium (International) on Combustion*, Pittsburgh, 1996.
(26) Glicker, S.; Okabe, H. *J. Phys. Chem.* **1987**, *91*, 437.
(27) Bandy, R. E.; Lakshminarayan, C.; Zwier, T. S. *J. Phys. Chem.* **1992**, *96*, 5337−5343.
(28) Allan, M. *J. Chem. Phys.* **1984**, *80*, 6020.
(29) Karpfen, A.; Lischka, H. *Chem. Phys.* **1986**, *102*, 91.
(30) Mahon, R.; Mcllrath, T. J.; Myerscough, V. P.; Koopman, D. W. *IEEE J. Quant. Electron.* **1979**, *6*, 444.
(31) Leopold, D. G.; Pendley, R. D.; Roebber, J. L.; Hemley, R. J.; Vaida, V. *J. Chem. Phys.* **1984**, *81*, 4218−29.
(32) Fahr, A.; Nayak, K. A. *Chem. Phys.* **1994**, *189*, 725−731.
(33) Arrington, C. A.; Zwier, T. S., unpublished results.
(34) Arrington, C. A.; Ramos, C.; Zwier, T. S., unpublished results.
(35) Knight, A. E. W.; Parmenter, C. S.; Schuyler, M. W. *J. Am. Chem. Soc.* **1975**, *97*, 1993−2005.
(36) Hollas, J. M.; Ridley, T. *J. Mol. Spectrosc.* **1981**, *89*, 232−253.
(37) King, G. W.; So, S. P. *J. Mol. Spectrosc.* **1971**, *37*, 543.
(38) Hagemeister, F. C.; Arrington, C. A.; Giles, B. J.; Quimpo, B.; Zhang, L.; Zwier, T. S. Cavity-Ring Down Methods for studying intramolecular and intermolecular dynamics. In *Cavity-Ring Down Spectroscopy*; Busch, K., Busch, M., Eds.; ACS Books: Washington, in press.
(39) Huntsman, W. D.; Chen, J. P.; Yelekci, K.; Yin, T.-K.; Zhang, L. J. *J. Org. Chem.* **1988**, *53*, 4357−4363.